

Forced Magnetic Reconnection Modeling with NIMROD

Matt Beidler

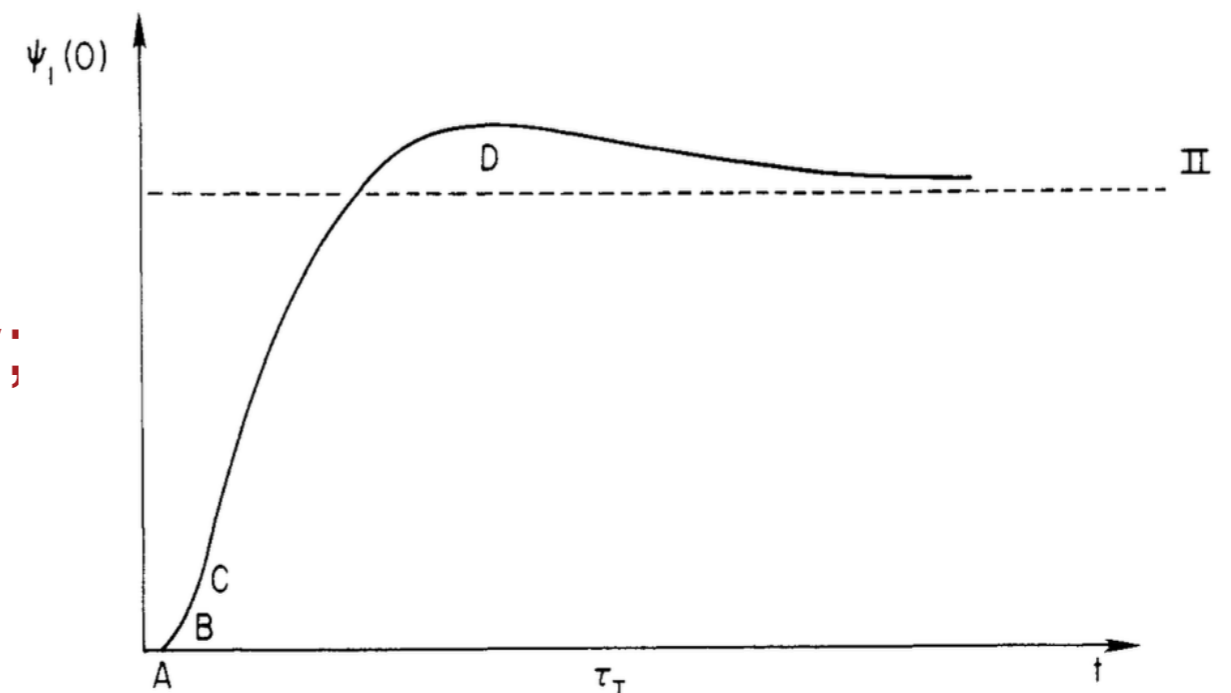
University of Wisconsin - Madison
CEMM Meeting: April 3, 2016

Acknowledging:

Jim Callen, Chris Hegna, Carl Sovinec,
Andi Becerra, Kyle Bunkers, and Eric Howell

Motivation is Verification of Forced Magnetic Reconnection Physics

- RMPs modify the magnetic field at the top of the H-mode pedestal; additional work is needed to understand their role in suppressing or mitigating ELMs
- Benchmarking of **forced magnetic reconnection (FMR)** with NIMROD and M3D-C¹ is needed to understand general linear and nonlinear responses to applied fields
- FMR in slab and cylindrical geometry is well understood analytically [e.g. Hahm and Kulsrud (1985)] and numerically; verification exercise with NIMROD is necessary before moving on to toroidal problem



We Use the NIMROD Code to Solve the Resistive-MHD Equations

- NIMROD capable of solving extended-MHD equations

$$\frac{\partial \mathbf{B}}{\partial t} = -\nabla \times \mathbf{E} + \kappa_{divb} \nabla \nabla \cdot \mathbf{B}$$

- Assume $\beta = 0$ in the following

$$\mathbf{E} = -\mathbf{V} \times \mathbf{B} + \eta \mathbf{J}$$

$$\mu_0 \mathbf{J} = \nabla \times \mathbf{B}$$

- Semi-implicit leapfrog time evolution is used:

$$\frac{\partial n}{\partial t} + \nabla \cdot (n \mathbf{V}) = \nabla \cdot D \nabla n$$

- Hold equilibrium fields constant and evolve perturbation fields

$$\rho \left(\frac{\partial \mathbf{V}}{\partial t} + \mathbf{V} \cdot \nabla \mathbf{V} \right) = \mathbf{J} \times \mathbf{B} + \nabla \cdot \nu \rho \nabla \mathbf{V}$$

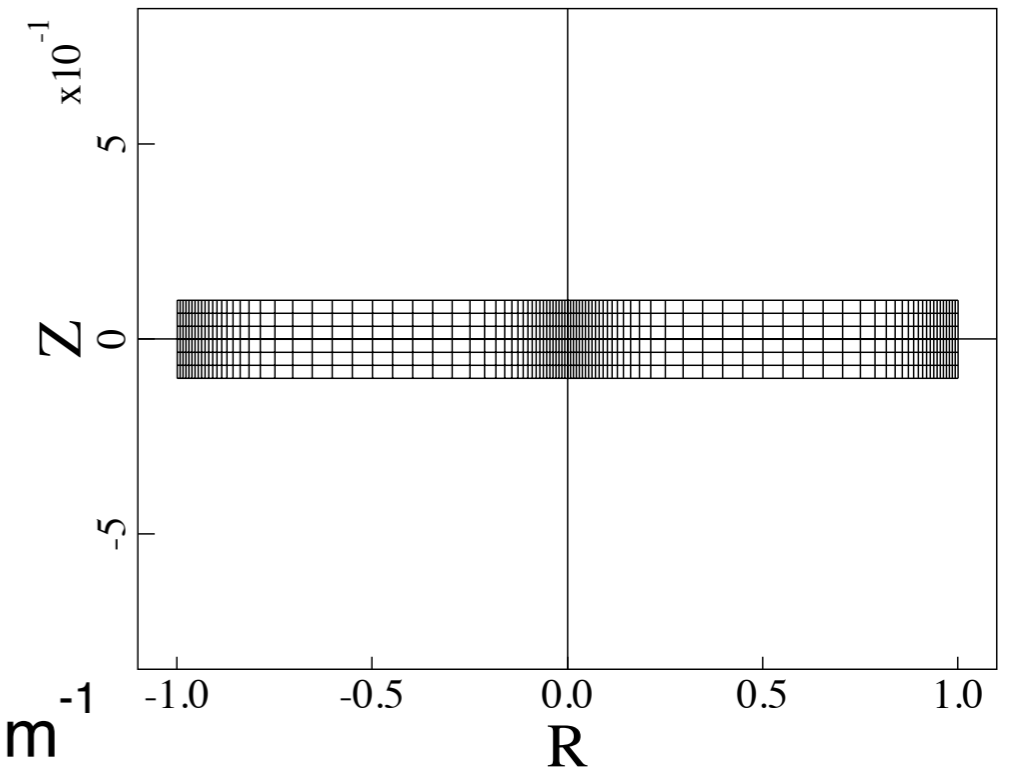
- Uses 2-D C^0 finite elements with Fourier decomposition in third dimension: $\mathbf{A}(R, Z, \phi) = \mathbf{A}_0 + \sum_{n=1} \mathbf{A}_n(R, Z) e^{in\phi} + \mathbf{A}_n^*(R, Z) e^{-in\phi}$

- Expansion coefficients of perturbation fields are complex

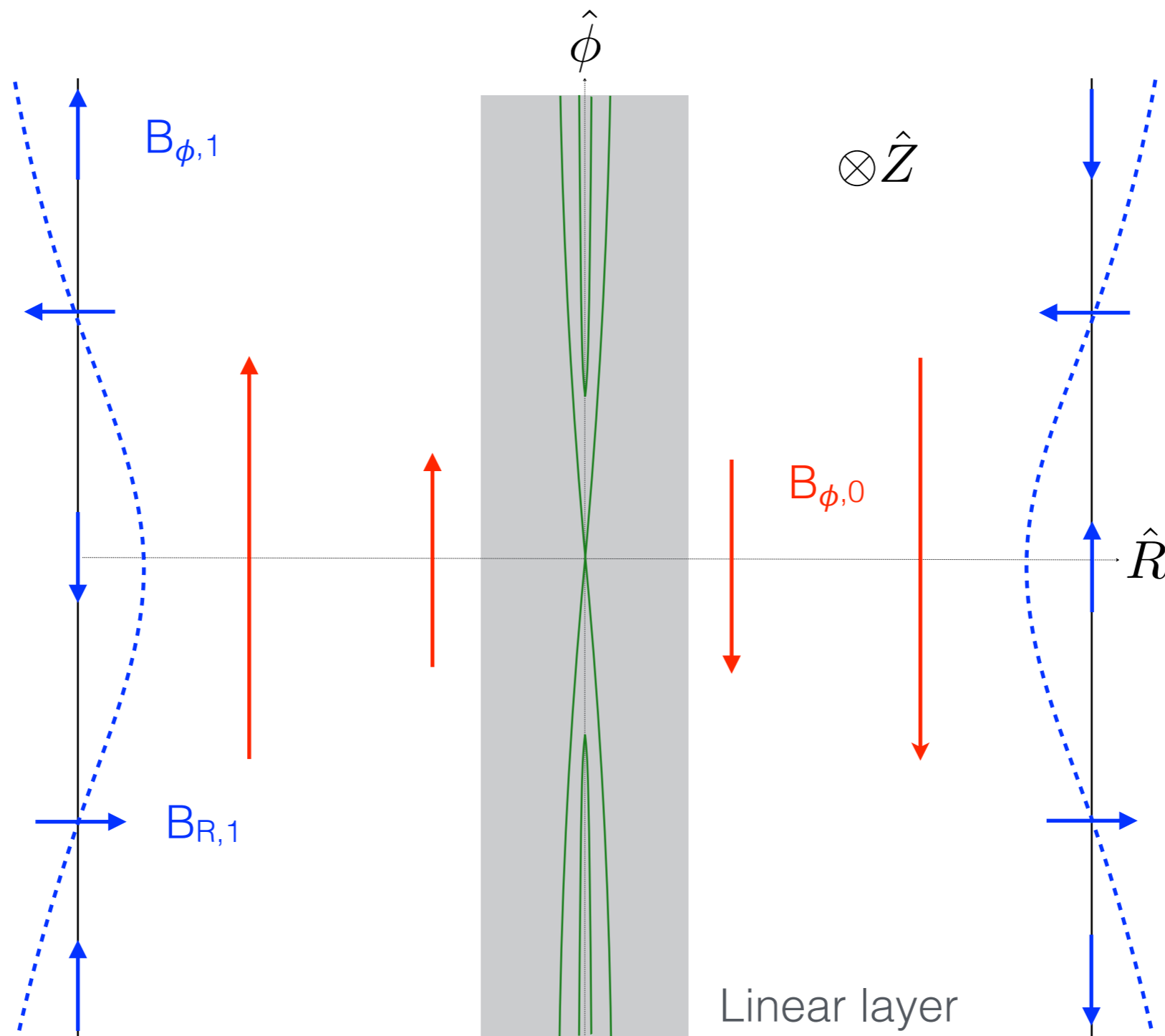
Many Parameters Are Specified For NIMROD Modeling

- R, Z, ϕ coordinates with $(L_R, L_Z) = (2*a = 2 \text{ m}, 0.2 \text{ m})$, $(n_R, n_Z) = (96, 6)$, and FEs with a polynomial degree of 4
 - 2-D reconnection with symmetric Z direction
 - Grid packing at boundary and rational surface with minimum grid (node spacing) $\approx 7.5 \times 10^{-3} \text{ m}$ ($1.9 \times 10^{-3} \text{ m}$)
- Periodic length of $L_\phi = 2 \text{ m}$
 - $n_\phi = 1$ linear calculations have $k_\phi \equiv 2\pi n_\phi / L_\phi = \pi \text{ m}^{-1}$
- $B_{z,0} = 10 \text{ T}$, $B_{\phi,0} = 0.1 \text{ T}$, $\Delta' = -2\pi$
 - $\tau_A \equiv a * (B_{\phi,0}^2 / \mu_0 \rho)^{1/2} = 1.45 \times 10^{-6} \text{ s} \rightarrow dt = 10^{-6} \text{ s}$
- Initial simulation uses $\eta / \mu_0 = 2 \text{ m}^2 / \text{s}$, $\nu = 0.002 \text{ m}^2 / \text{s}$
 - $\rightarrow P \equiv \tau_R / \tau_V = 10^{-3}$ [$\tau_R \equiv a^2 / (\eta / \mu_0)$, $\tau_V \equiv a^2 / \nu$], $S \equiv \tau_R / \tau_A = 3.45 \times 10^5$
 - \rightarrow Linear layer width $\sim a * S^{-1/3} P^{1/6} = 4.5 \times 10^{-3} \text{ m}$, calculated island half-width $\sim 1.05 \times 10^{-3} \text{ m}$

Finite Element Mesh

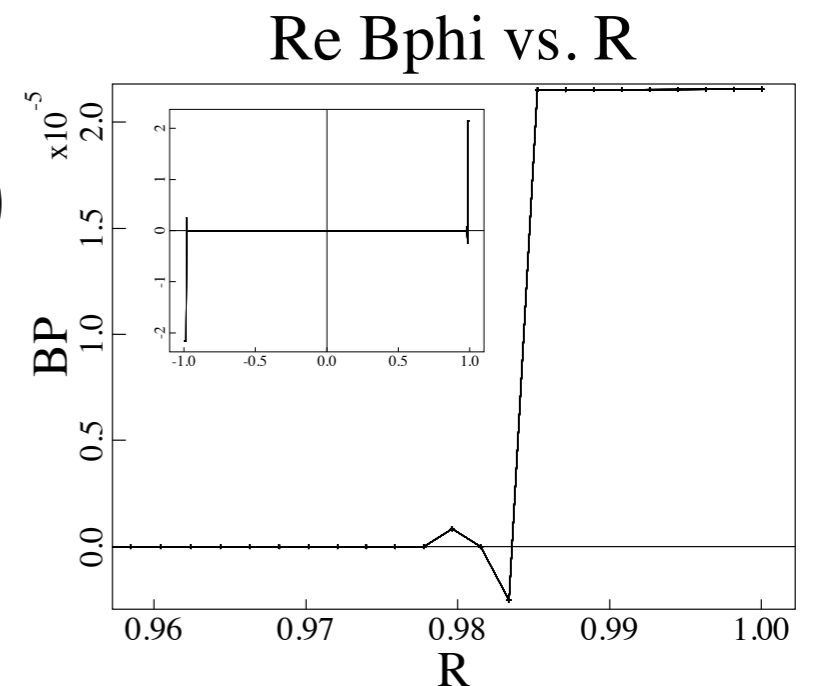
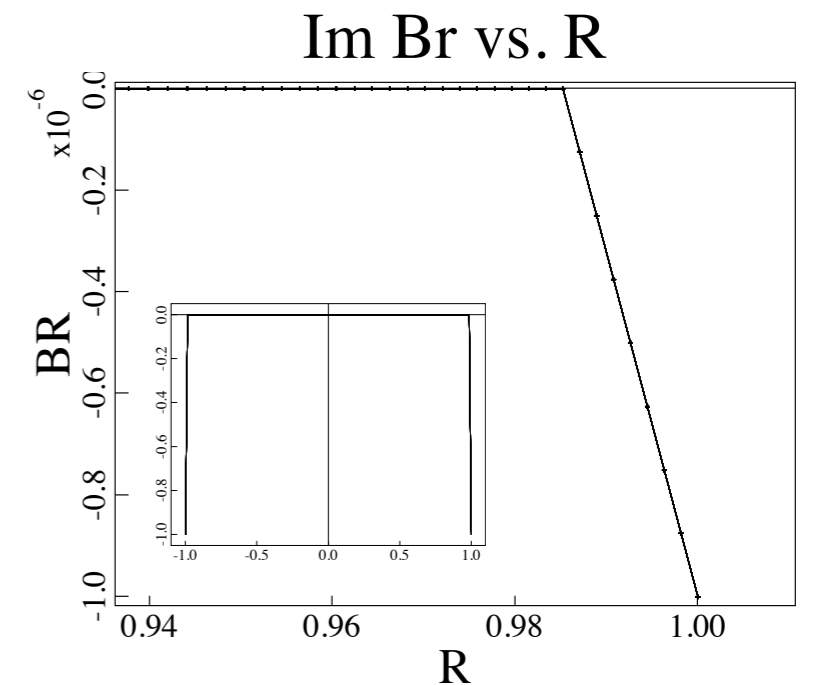


Paradigm Is Taylor's Slab Model Problem: Apply Edge Magnetic Field Perturbation



Boundary Perturbation Is Implemented In Two Edge Grid Points

- Solve vacuum (no plasma, currents) boundary-value problem in *edge region*
 - $\nabla^2 \varphi_1(R, \phi) = 0$ for perturbed $\mathbf{B}_{\perp,1} = -\nabla \varphi_1$
 - Two outermost grid cells of width Δ
 - $\mathbf{B}_{R,1}(a, \phi) = -iB_{nw}\xi(\phi)$, $\mathbf{B}_{R,1}(a-\Delta, \phi) = 0$
 - B_{nw} is the normal component of the magnetic field at the radial boundary
- $\varphi_1(R, \phi) = \frac{B_{nw}}{k_\phi} \frac{\cosh[k_\phi(R - a + \Delta)]}{\sinh(k_\phi \Delta)} (ie^{ik_\phi \phi} - ie^{-ik_\phi \phi})$
- HK δ is consistent with $\delta = B_{nw}/B_{\phi,0}k_\phi$
 - Initial linear simulation uses $B_{nw} = 10^{-6} \text{ T}$ ($\delta \sim 3.2 \times 10^{-6} \text{ m}$), which avoids nonlinear forcing



NIMROD Linear Results for Small Perturbation ($B_{nw} = 10^{-6}$ T) Are Close To HK Predictions

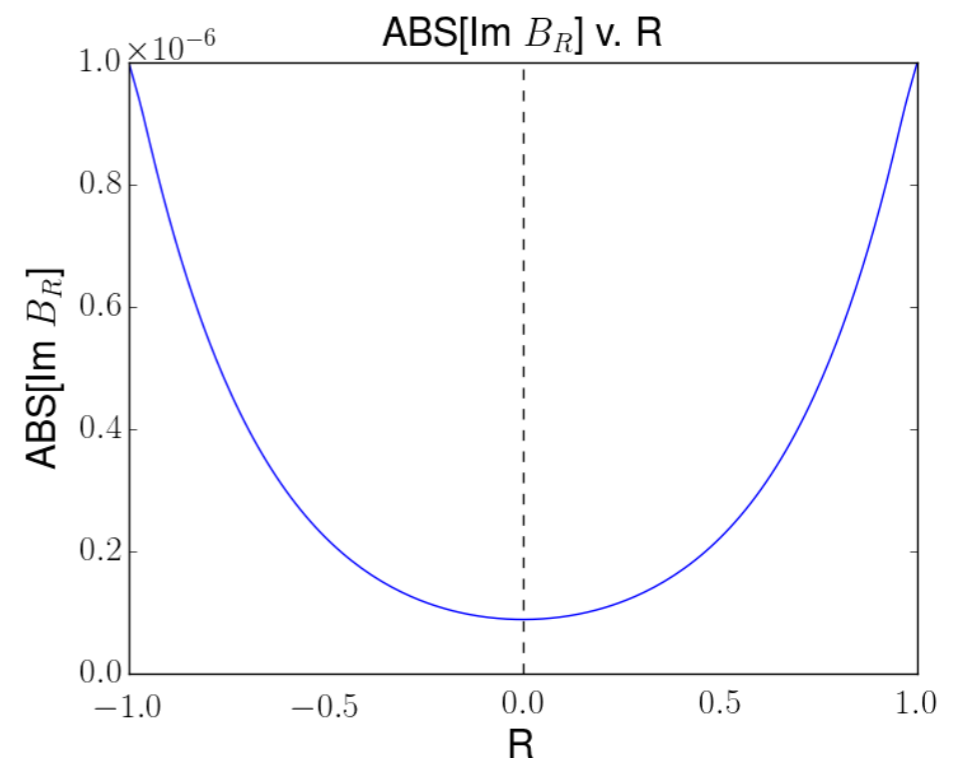
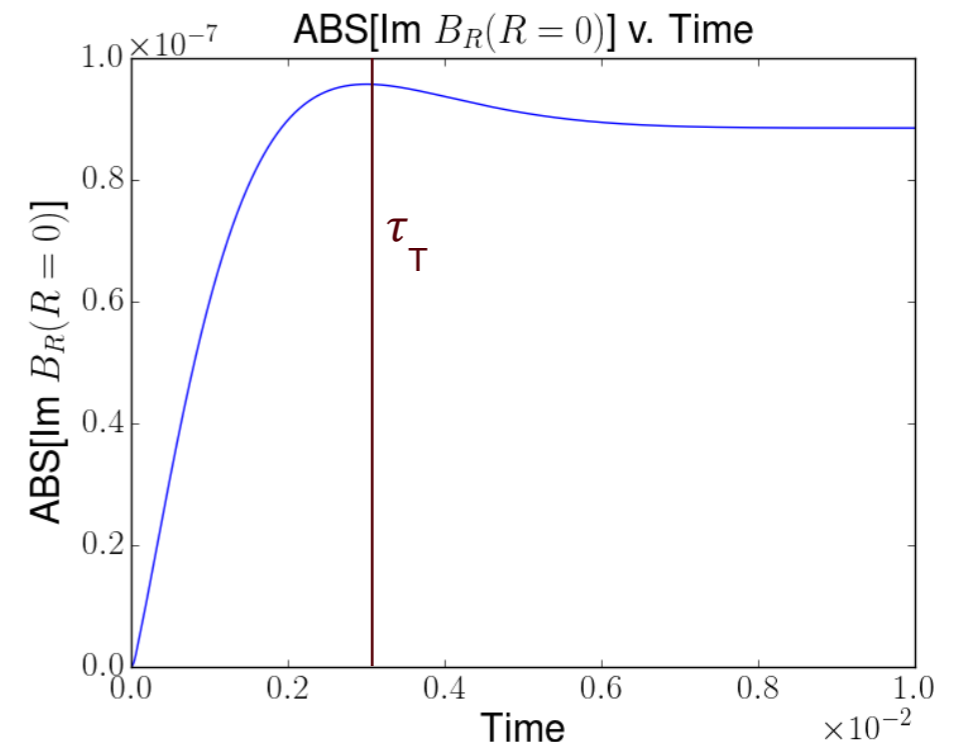
- Clearly observe overshoot in $B_{R,1}(R=0)$ evolution in top plot at $\tau_T = 3.05 \times 10^{-3}$ s
 - $B_{R,1}(R=0,t) \sim t^{1.22}$ (HK $\sim t^{5/4}$) for $t \ll \tau_T$
- For sheet pinch with constant current, HK showed that force balance reduces to vacuum boundary-value problem

- $\mathbf{B}_\perp = \hat{\mathbf{z}} \times \nabla \psi$ and BC $\psi_1(R=a) = B_{nw}/k_\phi$
- Solution for system with $\psi_1(R=0) \neq 0$ (i.e. resistive evolution):

$$\psi_1(R, \phi) = \frac{-B_{nw}}{k_\phi} \frac{\cosh(k_\phi R)}{\cosh(k_\phi a)} (e^{ik_\phi \phi} + e^{-ik_\phi \phi})$$

- $B_{R,1}(\phi=0) = -iB_{nw}^* [\cosh(k_\phi R)/\cosh(k_\phi a)]$

 - Predict $\text{Im}[B_{R,1}(R=0)] = -8.63 \times 10^{-8}$ T,
measure -8.85×10^{-8} T

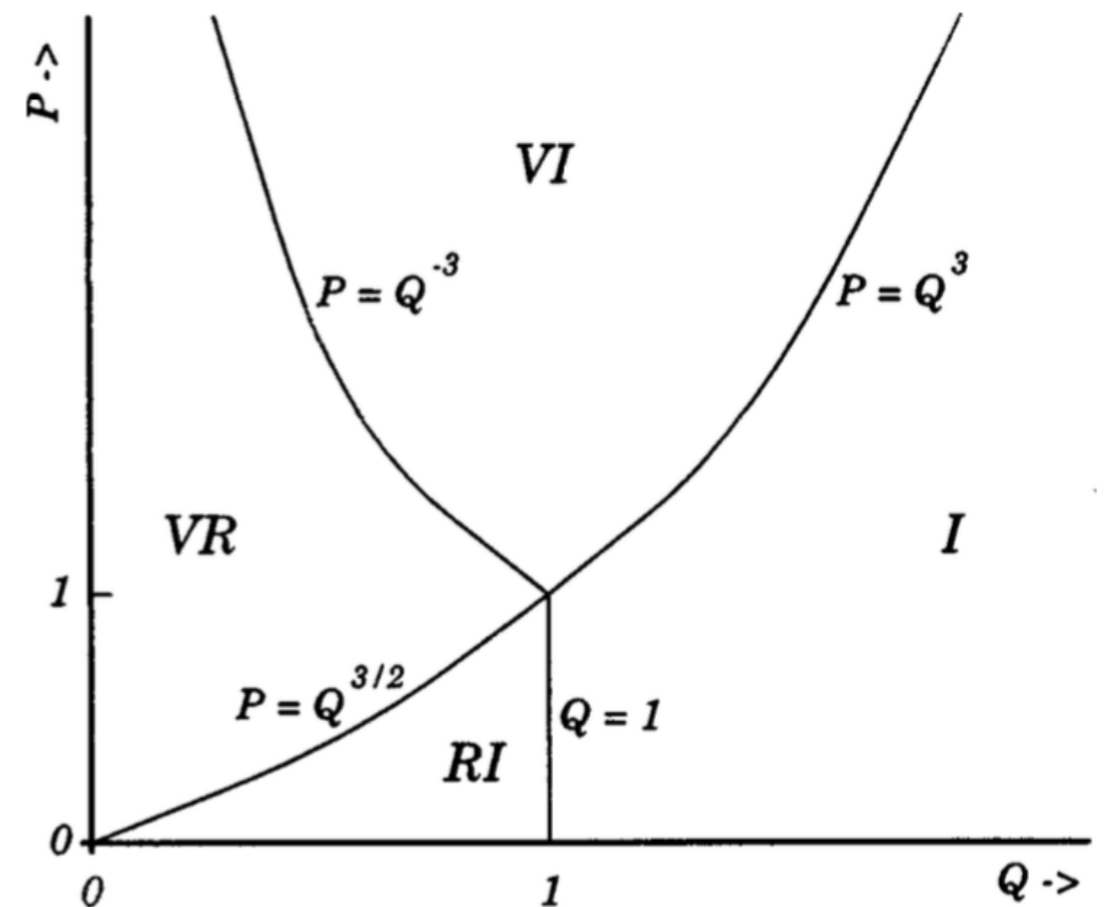


Equilibrium Flow Introduces Field Screening Physics

- Flows generate eddy currents that suppress tearing process
- Scaling with magnitude of flow is highly dependent upon layer physics [e.g. Fitzpatrick, POP (1998)]

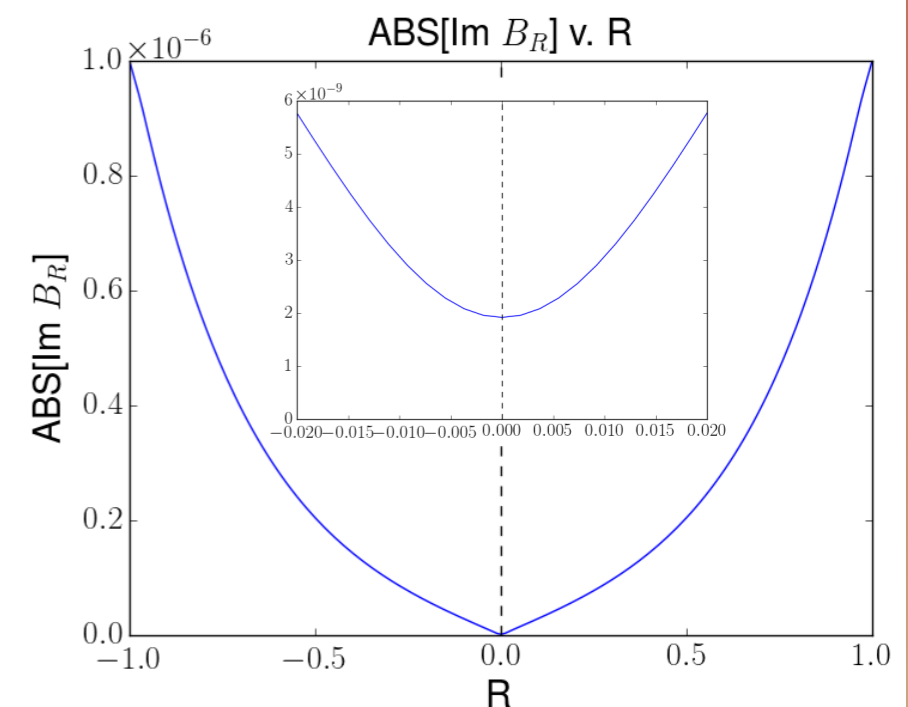
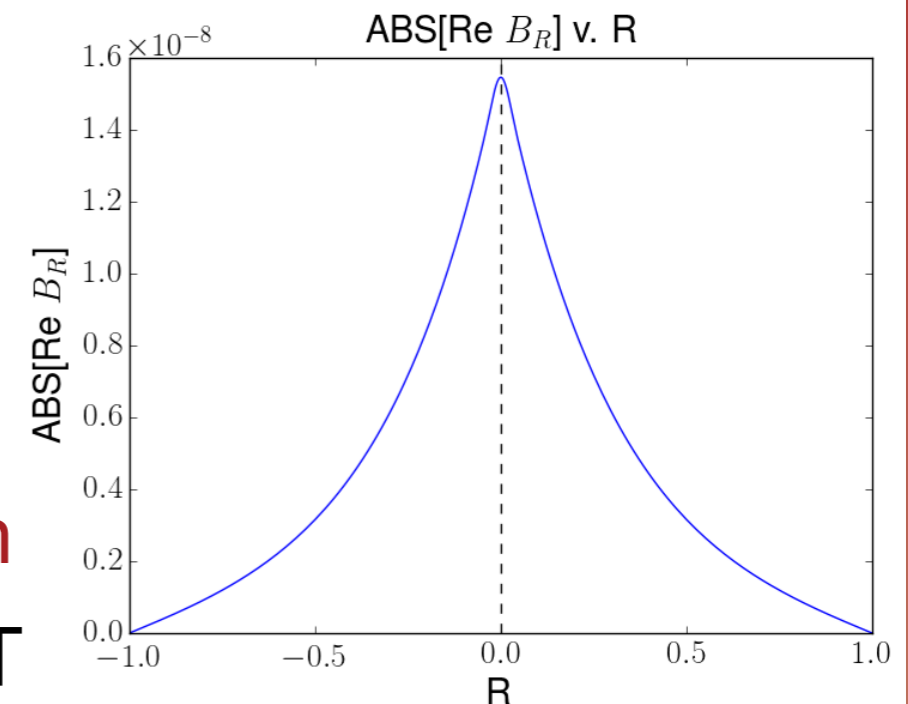
$$B_{norm} = \frac{1}{-\Delta' + \Delta(\omega)} \frac{2k_\phi}{\cosh(k_\phi a)} B_{nw}$$

- B_{norm} is $B_{R,1}$ at rational surface
- Form of $\Delta(\omega)$ depends on relative values of Prandtl number $P = \tau_R/\tau_V$ and normalized “slip frequency” $Q = \tau_A S^{1/3} \omega$, where $\omega = k_\phi v_\phi$
- P-Q space splits into 4 regimes: Resistive-Inertial (RI), **Visco-Resistive (VR)**, Visco-Inertial (VI), and Inertial (I)



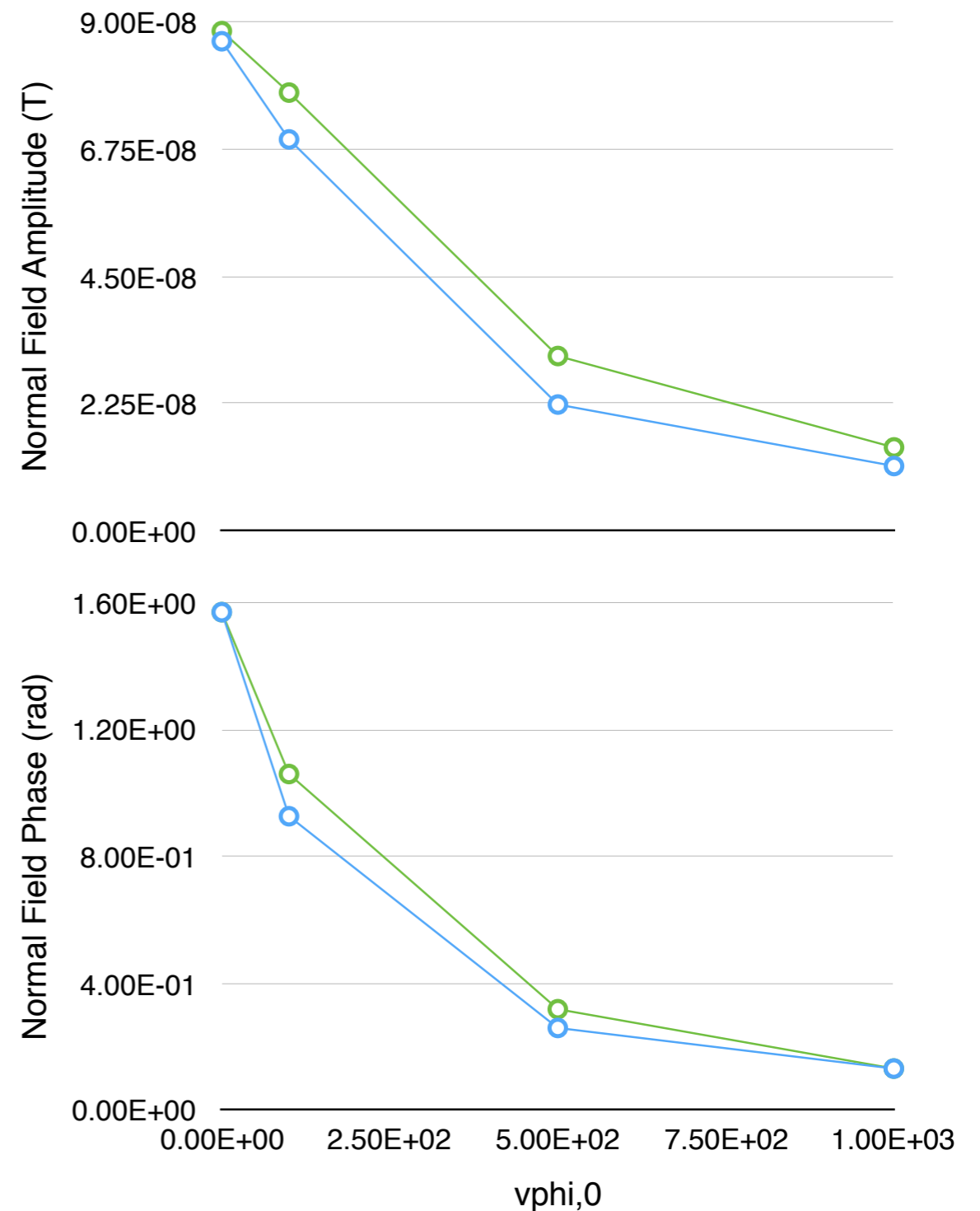
VR Regime Asymptotic State Agrees Well With Fitzpatrick Predictions

- With $P = 1$ and $v_{\phi,0} = 10^3$ m/s : $\text{Re}(Q) = 0.319$
 → In the VR regime
- VR regime has $\Delta(\omega) = i 2.104 \omega \tau_A a^{-1} S^{2/3} P^{1/6}$
 - $\omega \sim v_{\phi}$ is complex, with imaginary component due to Fourier decomposition
- Theory predicts $\text{Re}[B_{R,1}(R=0)] = -1.16 \times 10^{-8}$ T and $\text{Im}[B_{R,1}(R=0)] = -1.54 \times 10^{-9}$ T
 - Numerically within $\sim 25\%$ of predictions
- Increasing $v_{\phi,0}$ parallel to $B_{\phi,0}$ decreases the magnitude of the normal field at the rational surface (*smaller islands*)
 - Also shifts island along direction of flow



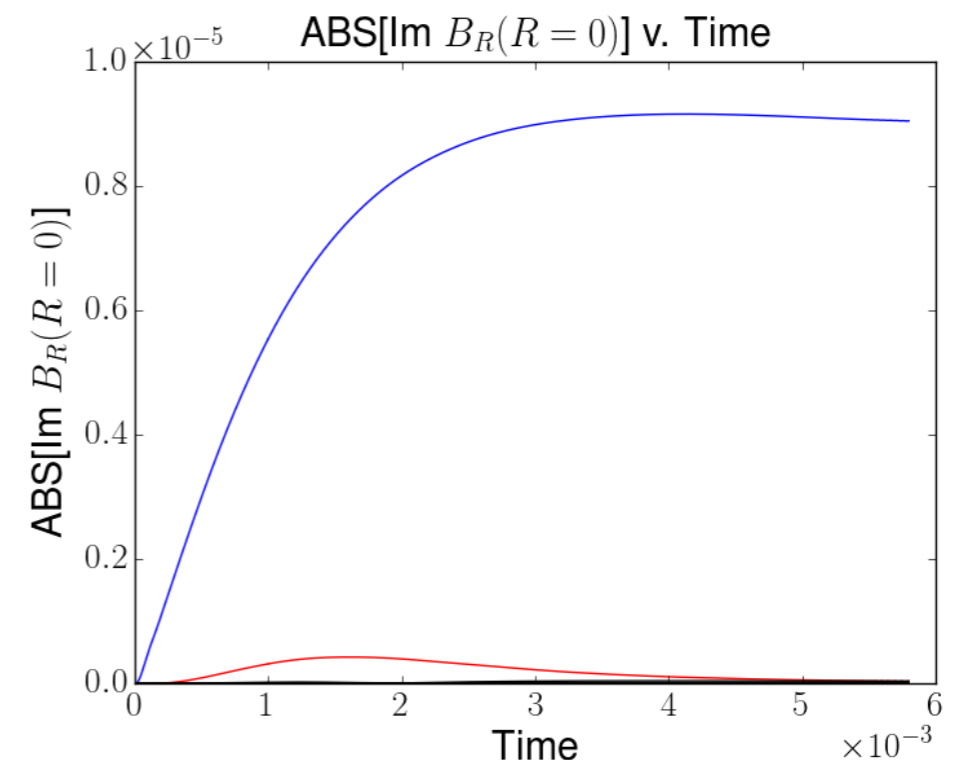
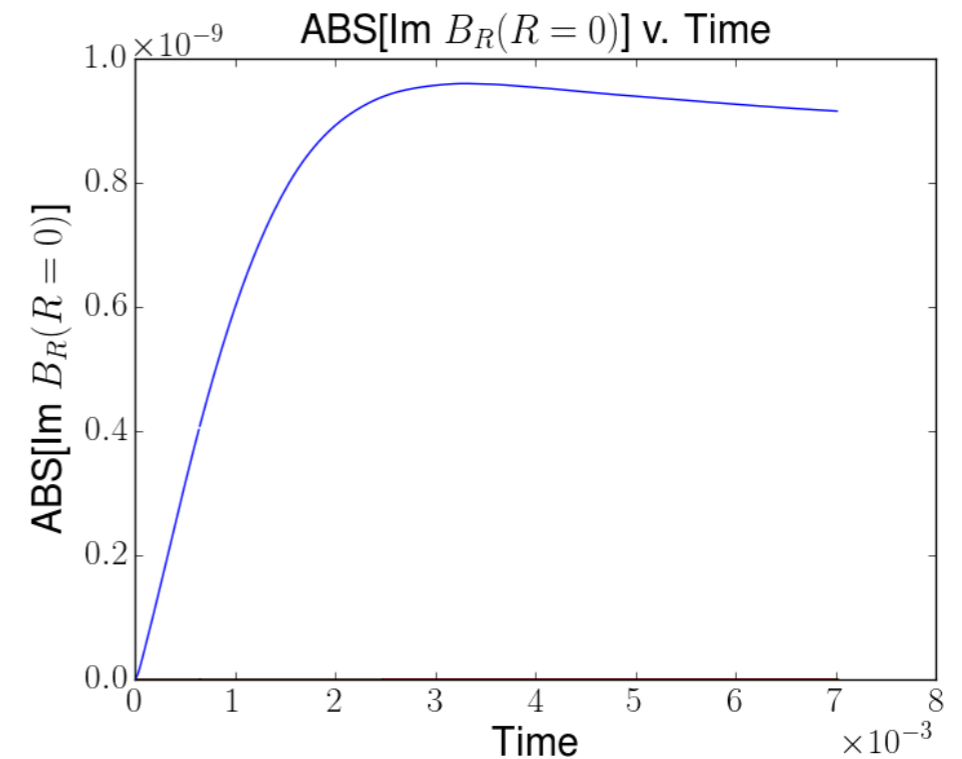
Scaling with Flow Follows Fitzpatrick's Results

- Magnitude (top) and phase (bottom) of normal field as equilibrium flow is varied in the VR regime
 - Blue data correspond to analytically predicted values from Fitzpatrick POP (1998)
 - Green data correspond to numerically observed values
- NIMROD slightly over predicts the magnitude and under predicts the phase shift as the flow is increased



Larger Amplitude Boundary Perturbation ($B_{nw} = 10^{-4}$ T) Causes Nonlinear Forcing

- Nonlinear simulations keep $n_\phi = 0 - 5$
 - Increased polynomial degree and edge viscosity to improve convergence
 - Turned off density evolution
- Top: $B_{nw} = 10^{-8}$ T
 - Resembles linear simulations
 - Early growth scales as $\sim t^{1.15}$ (HK $\sim t^{5/4}$)
- Bottom: $B_{nw} = 10^{-4}$ T
 - $n_\phi = 1$ mode evolution (blue trace) consistent with boundary-driven Rutherford evolution:
 - Early growth as $\sim t^{0.845}$ (HK $\sim t^{2/3}$)
 - Higher order modes (e.g. $n_\phi = 2$ red trace) observed on same scale



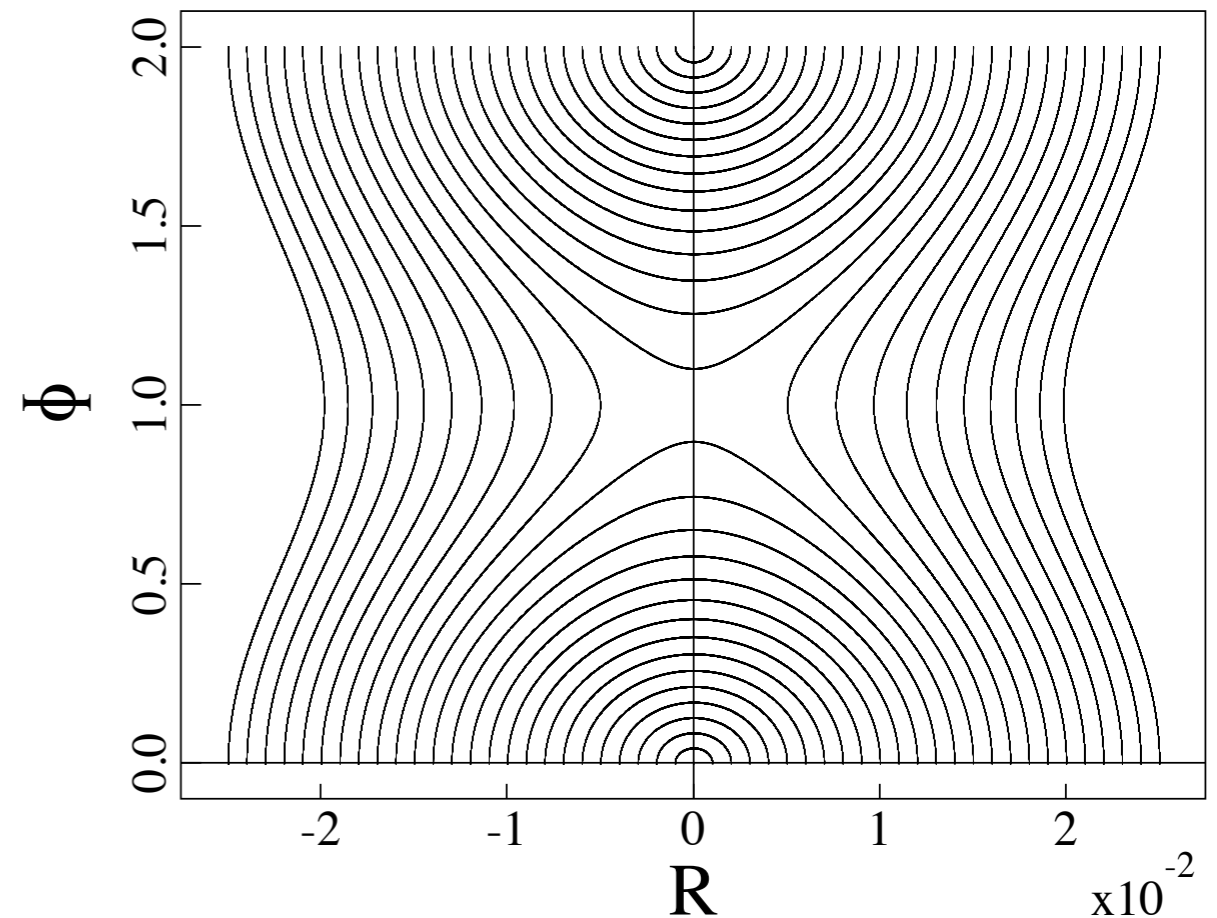
Nonlinear Driving Forms Large Island

- For $B_{nw} = 10^{-4} \text{ T}$ and $v_{\phi,0} = 0$, HK predicts a saturated island half-width of

$$\sqrt{\frac{4aB_{norm}}{B_{\phi,0}k_{\phi}}} = 1.05 \times 10^{-2} \text{ m}$$

- Appropriate for a visco-resistive linear layer width of $a^*S^{-1/3}P^{1/6} = 4.51 \times 10^{-3} \text{ m}$
- Observed island is $\sim 50\%$ wider than predicted
- Note the different scales of the R, Z axis distort the X-null and island structure appearance

Surface of Section



Nonlinear Electromagnetic and Viscous Force Balance Gives Rise to Bifurcation

- Integrating $\mathbf{J} \times \mathbf{B}$ and $\rho \nu \nabla^2 \mathbf{v}$ over ϕ and radially about the rational surface gives $n=0$ electromagnetic and viscous forces [e.g. Fitzpatrick NF (1993)]

$$\hat{F}_{\phi, EM} = \frac{2k_{\phi} L_{\phi}}{\mu_0 \cosh^2(k_{\phi} a)} \frac{\text{Im}[\Delta(\omega)]}{(-\Delta')^2 + |\Delta(\omega)|^2} B_{nw}^2$$

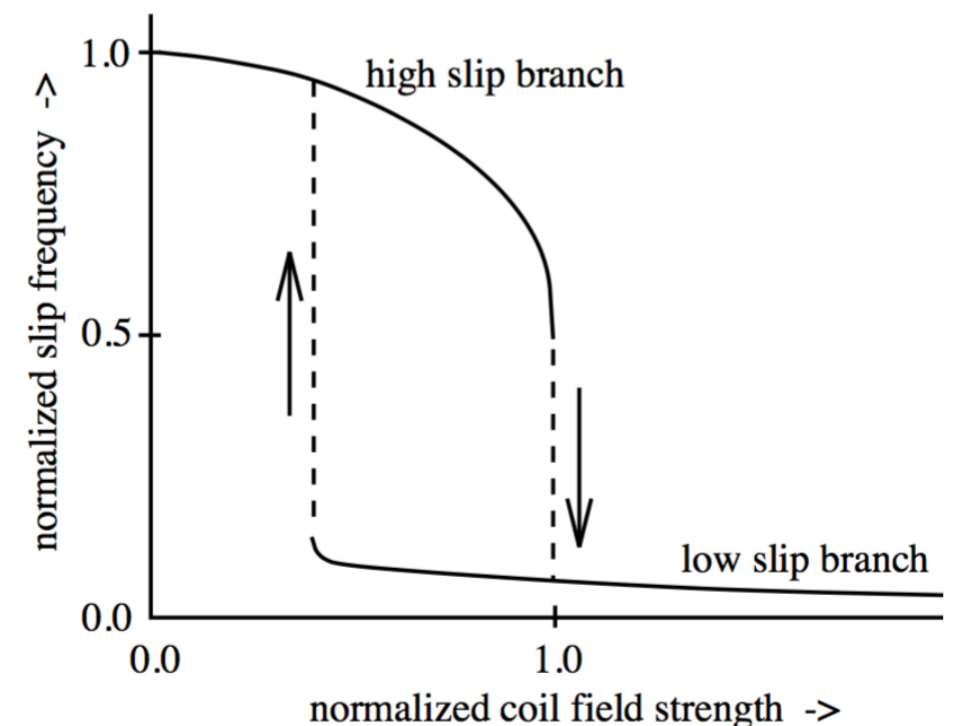
$$\hat{F}_{\phi, VS} = -\frac{L_{\phi}^2 \rho \nu}{n\pi a} (\omega_0 - \omega)$$

- Force balance gives cubic relation in ω

$$\frac{\omega_0}{\omega} - 1 + \omega_0 \omega \tau_L^{*2} - 2\omega^2 \tau_L^{*2} = \frac{\tau_L}{(-\Delta') \rho \nu} \frac{k_{\phi}^2}{\mu_0 \cosh^2(k_{\phi} a)} B_{nw}^2$$

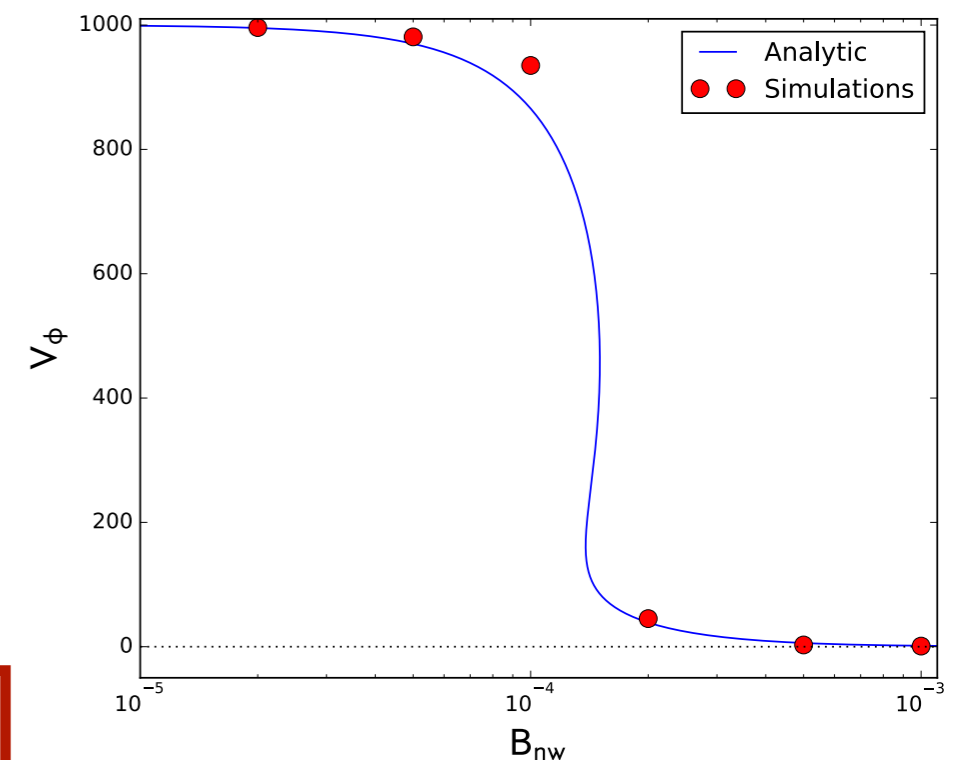
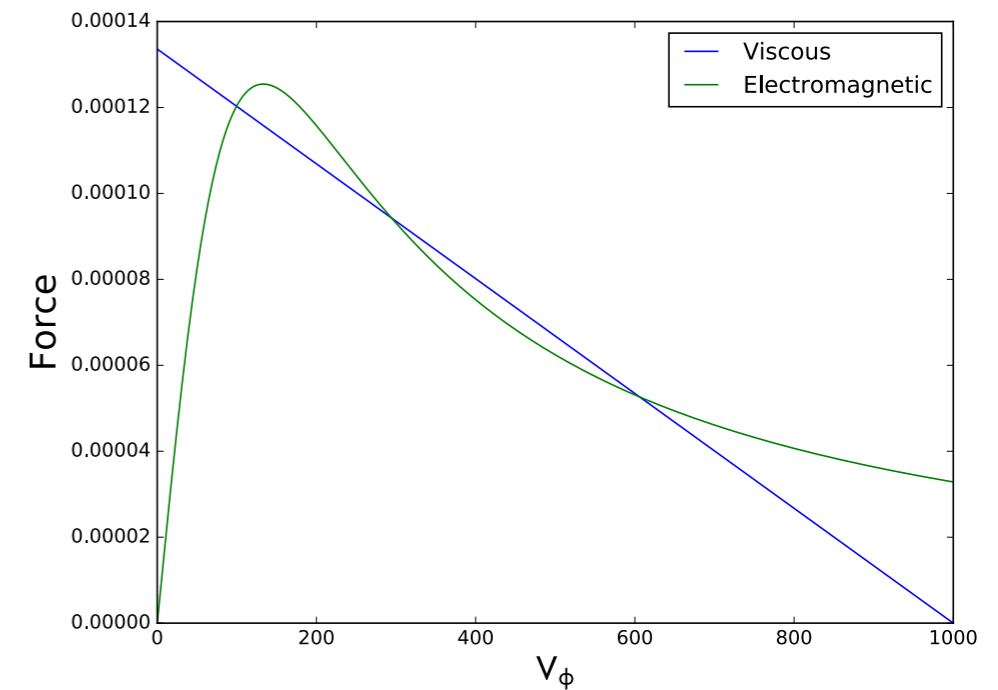
where $\tau_L = 2.104 \tau_A S^{2/3} P^{1/6}$ and $\tau_L^* = \frac{\tau_L}{a(-\Delta')}$

- Bifurcation when initial angular frequency exceeds $\omega_{0, crit} = \frac{3\sqrt{3}}{\tau_L^*}$



Force Balance Bifurcation is Numerically Observed in Asymptotic States

- Analytic, integrated, nonlinear EM (green) and viscous (blue) forces plotted in top figure
 - Both figures shown for $v_{\phi,0} = 10^3 \text{ m/s} > v_{0,\text{crit}} = 6.92 \times 10^2 \text{ m/s}$
 - Two stable (and one metastable) solutions exist, **high and low slip**
- Bottom figure shows cubic force balance equation in blue overlaid with asymptotic NIMROD results in red
 - **Simulations clearly show bifurcation**



High/Low Slip Solutions Have Reduced/Typical Islands

- High slip solution (top plot) has $B_{nw} = 10^{-4} \text{ T}$ and low slip solution (bottom plot) has $B_{nw} = 2 \times 10^{-4} \text{ T}$

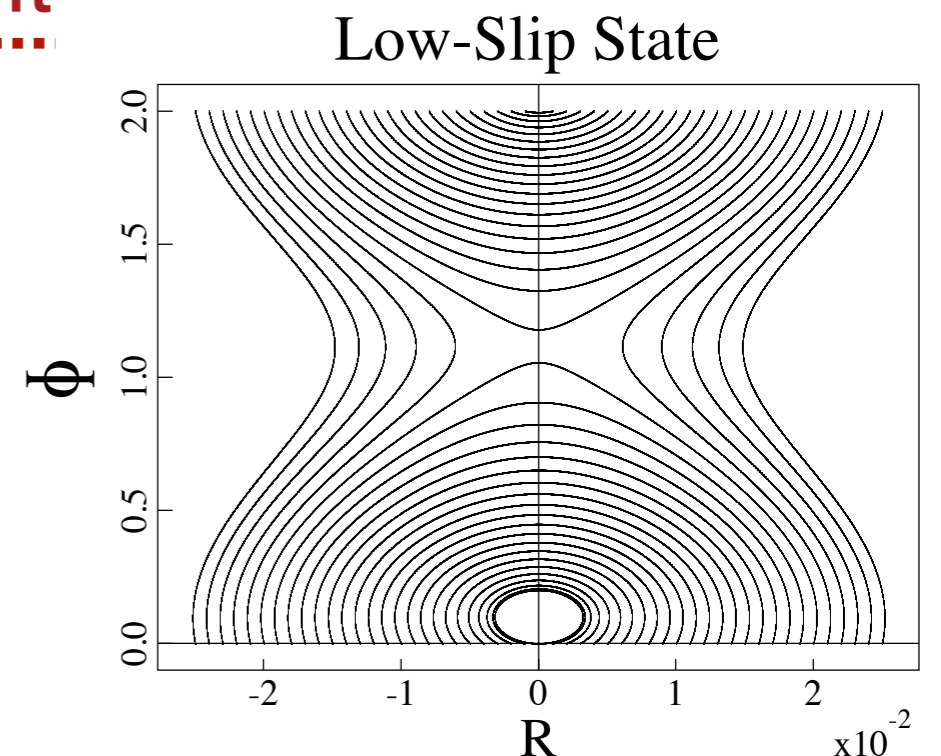
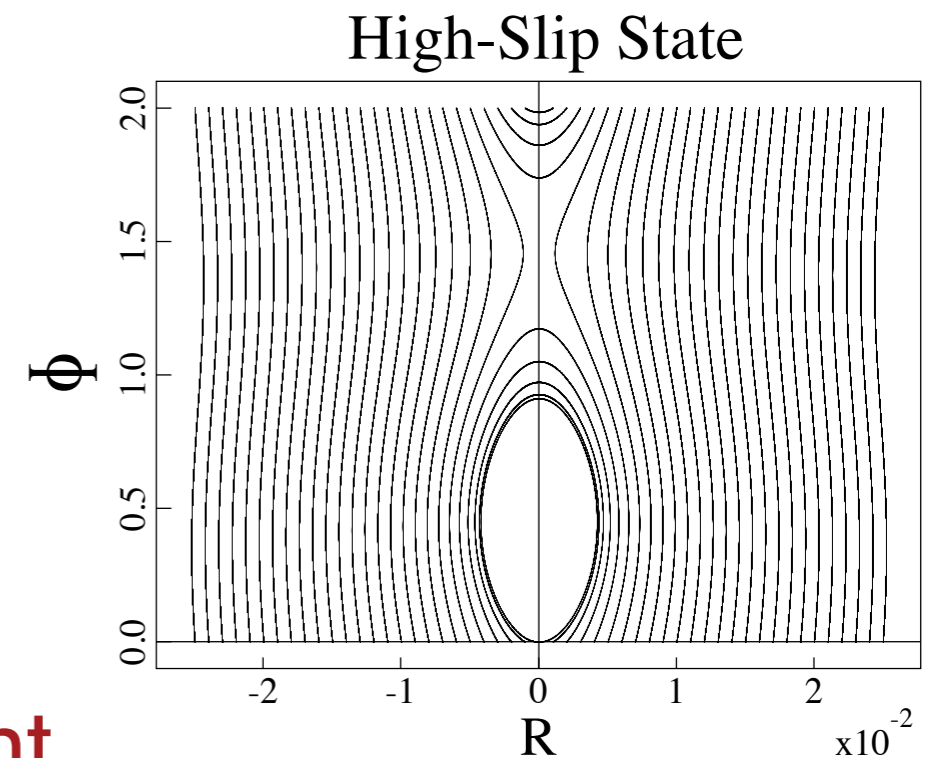
- Predicted island half-widths given by $\sqrt{\frac{4aB_{norm}}{k_{\phi}B_{\phi,0}}}$

- Takes flow screening into account

- Predict $4.54 \times 10^{-3} \text{ m}$ and $1.44 \times 10^{-2} \text{ m}$, respectively

- Measured island half-widths of $6.17 \times 10^{-3} \text{ m}$ and $2.07 \times 10^{-2} \text{ m}$

- Also observe flow shifting of island



FMR Simulations are Underway in the Cylindrical Geometry

- Specify q -profile according to Furth, Rutherford, and Selberg (1973) form

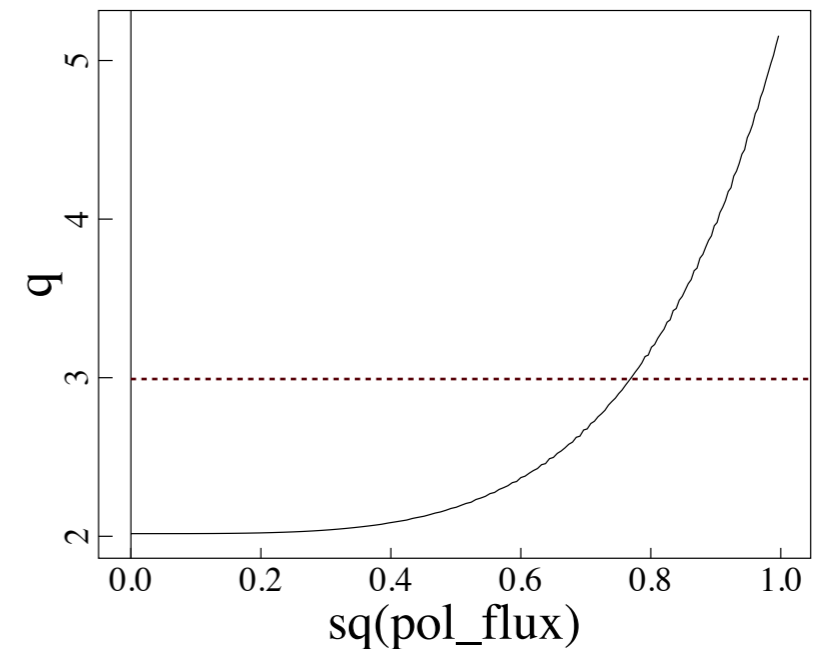
- $$q(r) = q_0 \left[1 + \left(\frac{r}{r_0} \right)^{2\lambda} \right]^{1/\lambda}$$

- $q_0 = 2.02, r_0 = 0.65, \lambda = 2$

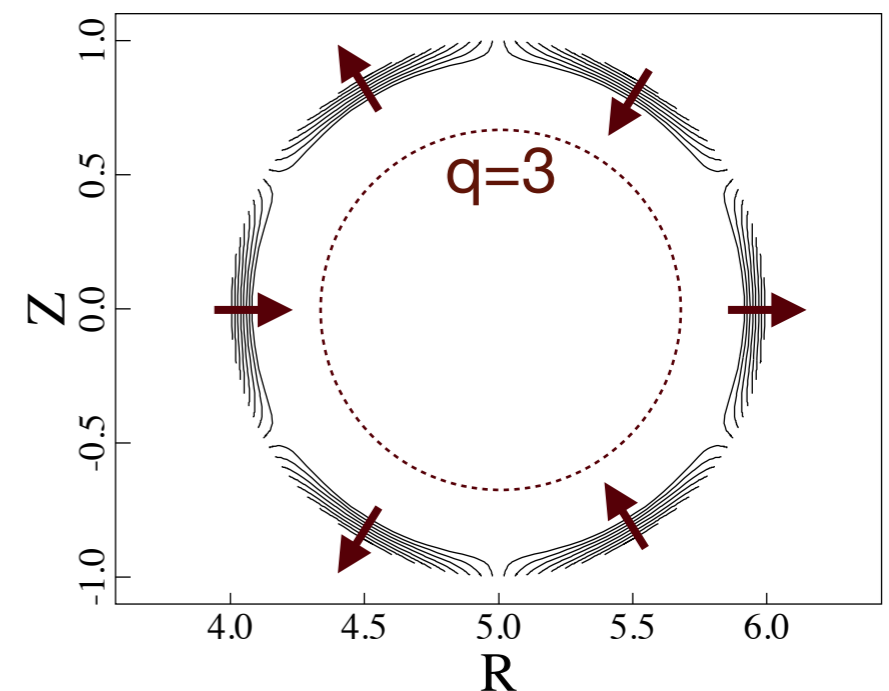
- $r(q=3) = 0.681 \text{ m}, \rho(q=3) = 0.796$

- $P = 1$ and similar S to slab case
- Follow same procedure as in slab geometry to prescribe edge boundary perturbation
 - Initialize $(m,n) = (-3,1)$ perturbation in linear $n=1$ simulations

q vs $\text{sq}(\text{pol_flux})$

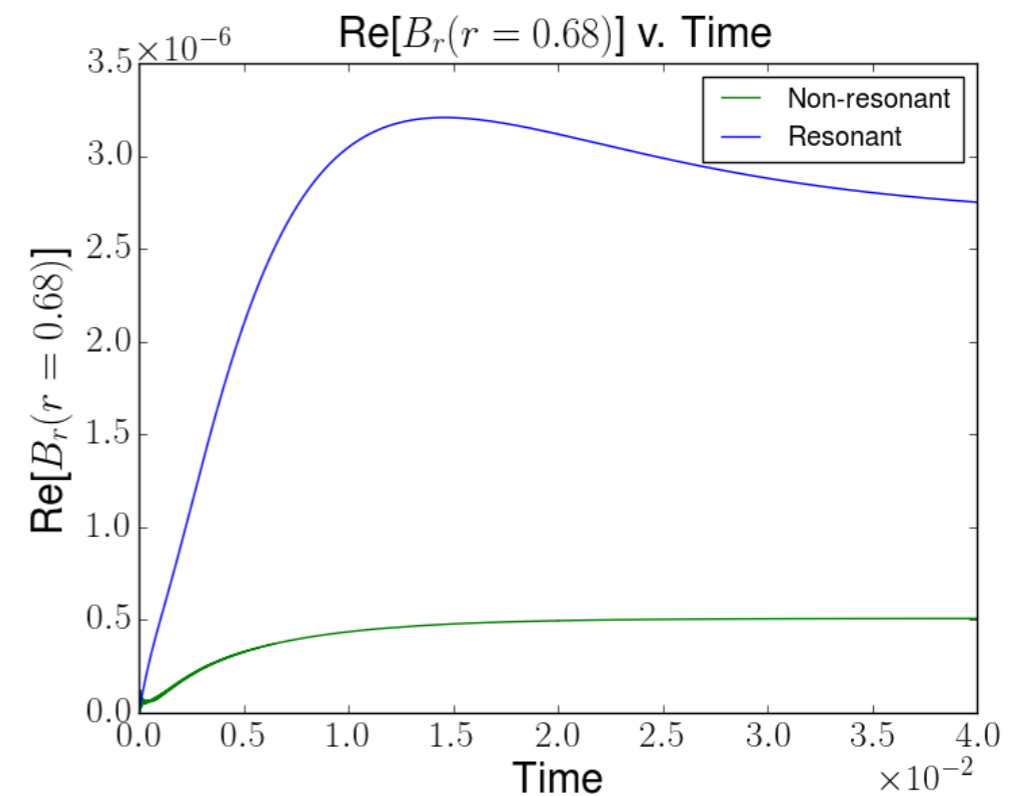


Re Br



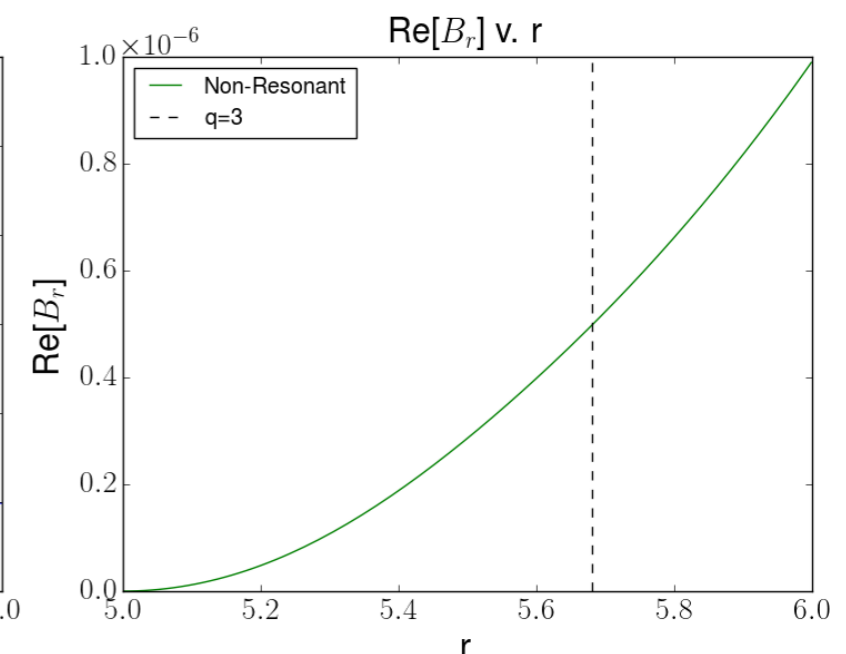
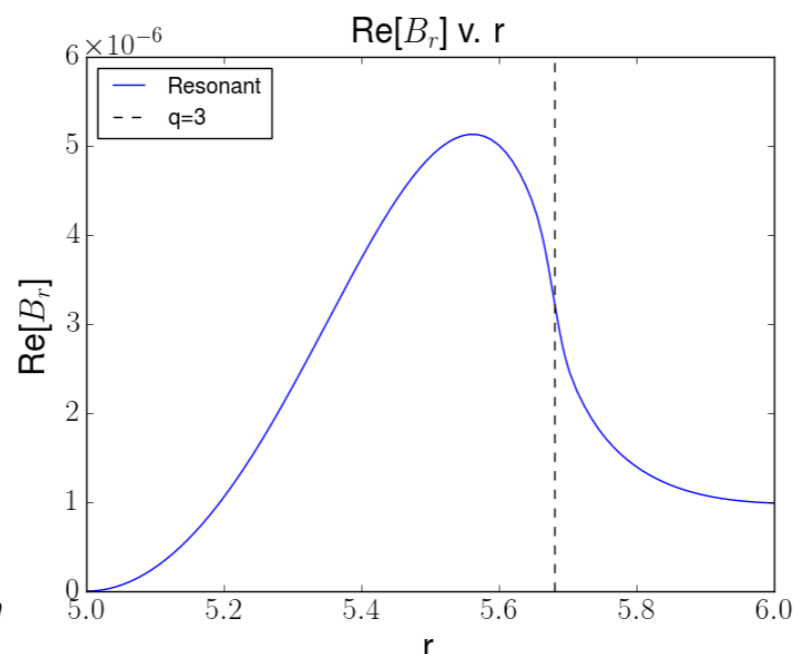
Resonant Perturbation Field in Cylinder Evolves Similar to HK Case

- $B_{nw} = 10^{-6}$ T edge perturbation triggers FMR when resonant with $q = 3$ surface (blue trace)
 - Plotting field at the rational surface on the outboard midplane
 - Cross-helicity case with $m = 3$ (green trace) diffuses inward on longer timescale



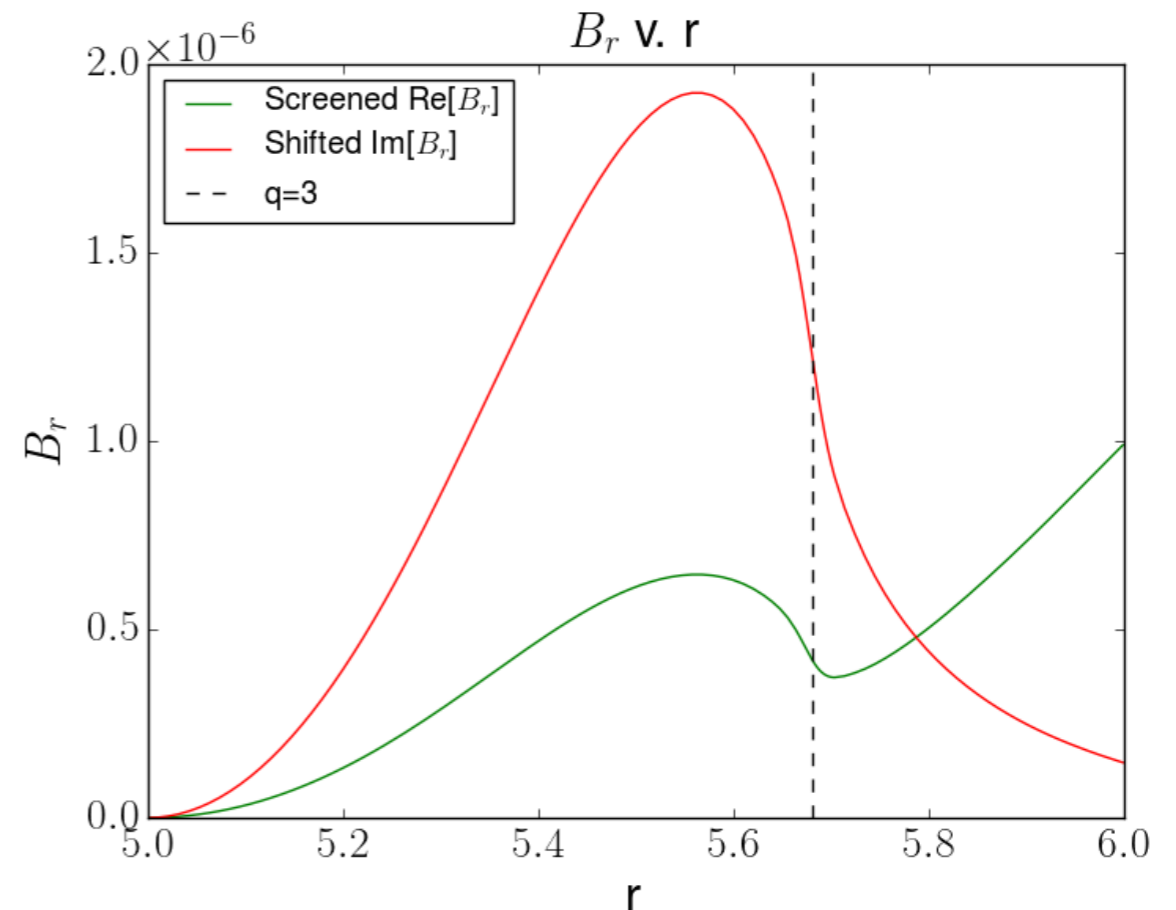
- Resonant field is amplified at rational surface with zero equilibrium flow

$$B_{norm} = \frac{2m}{-\Delta' + \Delta(\omega)} B_{nw}$$



Flow Screening Qualitatively Agrees with Fitzpatrick Predictions

- With $v_{\phi,0} = 10^3$ m/s, observe $\text{Re}[B_r(\theta=0)]$ is decreased (green trace) and $\text{Im}[B_r(\theta=0)]$ is now nonzero (red trace)
- Flow screens and shifts B_r
- As in slab, we are in VR regime
 - Theory predicts $\text{Re}[B_r(\theta=0)] = 1.03 \times 10^{-6}$ T and $\text{Im}[B_r(\theta=0)] = -1.53 \times 10^{-6}$ T
 - Note figure has $\text{ABS}[\text{Im}(B_r)]$
- Hypothesize discrepancy due to value of Δ' used in calculations



Future Direction Of This Research

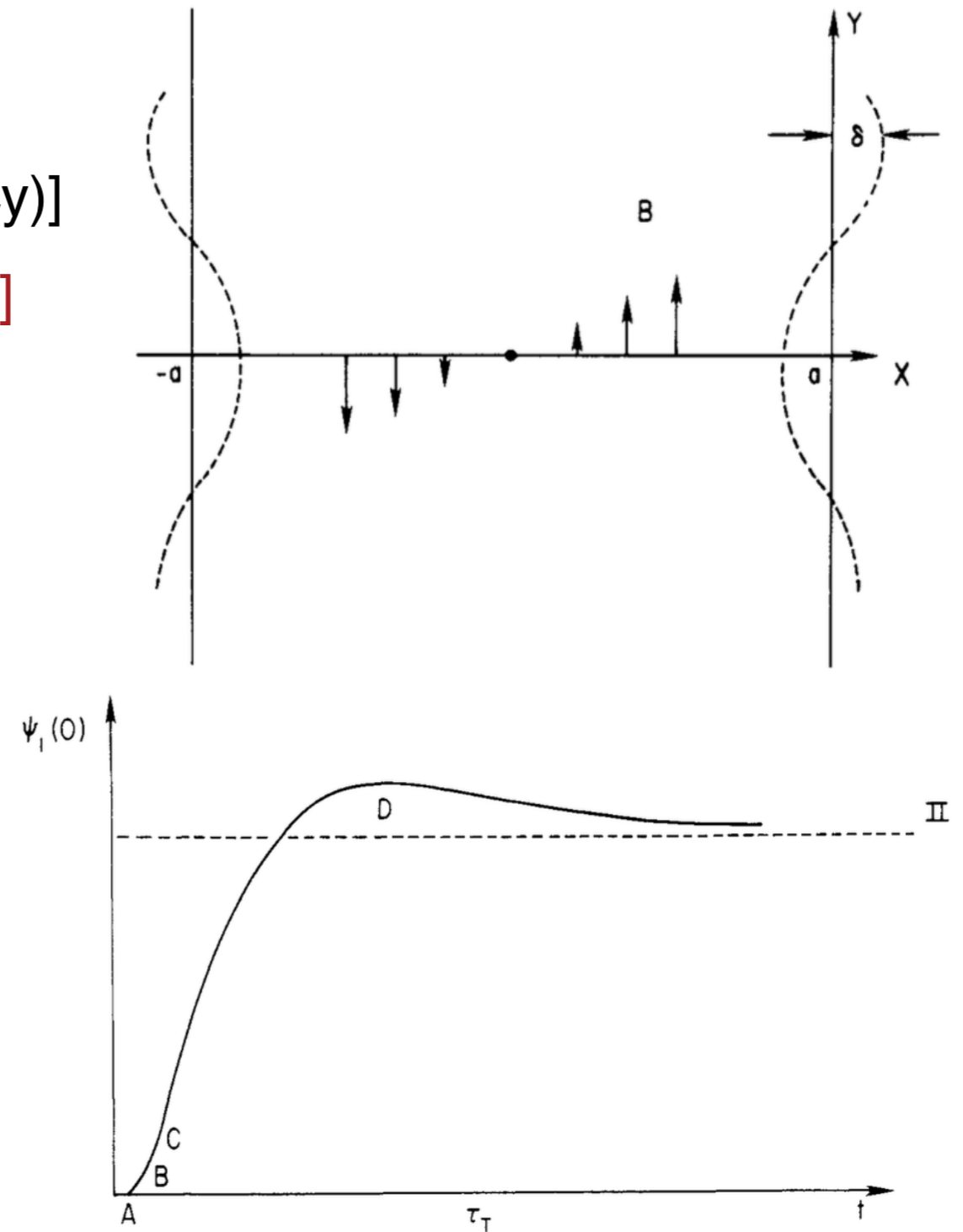
- *Trigger bifurcation* in slab by increasing edge field magnitude slowly compared to system evolution
 - Observe hysteresis by slowly decreasing edge field
- Linear and nonlinear flow-scaling in a cylinder
 - Torque balance bifurcation
- Linear and nonlinear flow-scaling in a torus with the addition of two-fluid effects
- **Benchmarks between NIMROD and M3D-C¹**

Conclusions

- Verified Hahm and Kulsrud analytical model of linear and nonlinear evolution of Taylor's problem by applying spatially-varying, boundary-normal magnetic field in NIMROD simulations
- Verified flow-screening effects consistent with Fitzpatrick model for linear slab, notably in the visco-resistive regime typical for tokamak H-mode pedestals
- Verified nonlinear force balance bifurcation consistent with Fitzpatrick model, that gave rise to high and low slip solutions
- Preliminary numerical study of FMR in cylindrical geometry is underway

Hahm & Kulsrud (HK) Slab Model Provides Paradigm Problem

- Taylor's problem: resistive sheet pinch with $\mathbf{B} = B_T \hat{\mathbf{z}} + (B_0/a)x\hat{\mathbf{y}}$
 - Boundaries perturbed by $x = \pm [a - \delta \cos(k_y y)]$
- Tearing creates magnetic islands [$\psi(x=0) \neq 0$] with finite resistivity
 - For resistive phase $t \ll \tau_{\text{Res}} \equiv \tau_A S^{1/3}$, $\psi(x=0, t) \sim t^2$
 - For tearing phase $t \sim \tau_T \equiv \tau_A S^{3/5}$, $\psi(x=0, t) \sim t^{5/4}$ for $t \ll \tau_T$ and $\psi(x=0, t) \sim t^{-5/4}$ for $t \gg \tau_T$
- Nonlinear driving when $\delta/a \geq S^{-4/5}$
 - For $t \ll \tau_{\text{NL}} \sim (\delta/a)^{1/2} \tau_R$, $\psi(x=0, t) \sim t^{2/3}$
 - For $t \gg \tau_{\text{NL}}$, $\psi(x=0, t) \sim \tanh^2(t/\tau_{\text{NL}})$



Time Asymptotic State Of Linear Results Agree with HK

- For sheet pinch with constant current in the symmetry direction, HK showed that force balance reduces to vacuum boundary-value problem

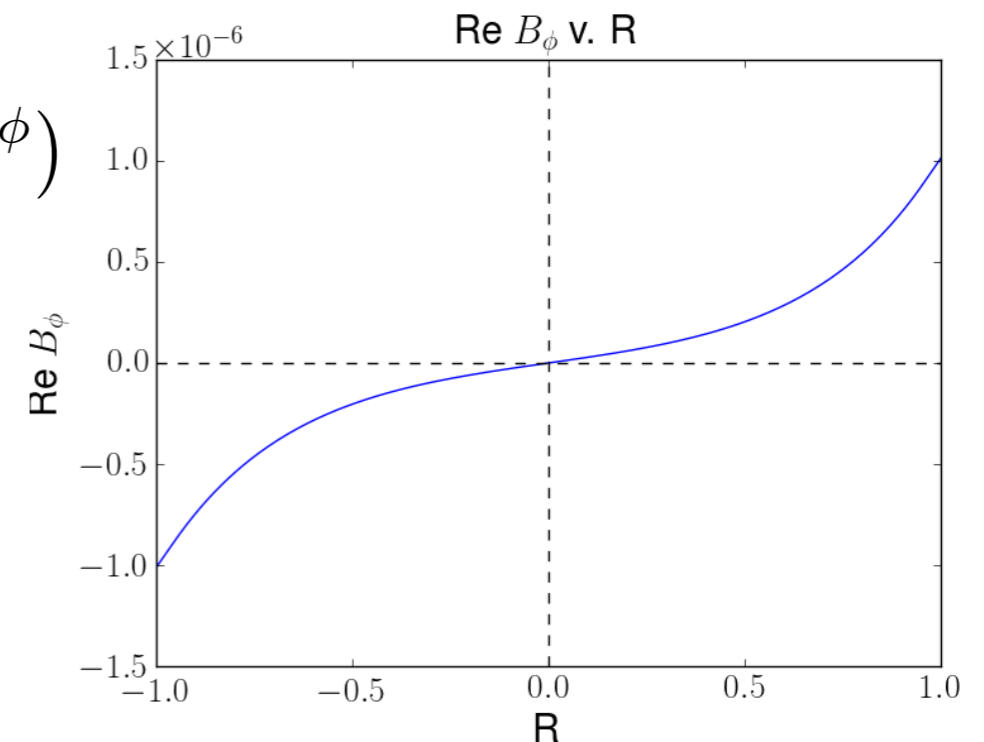
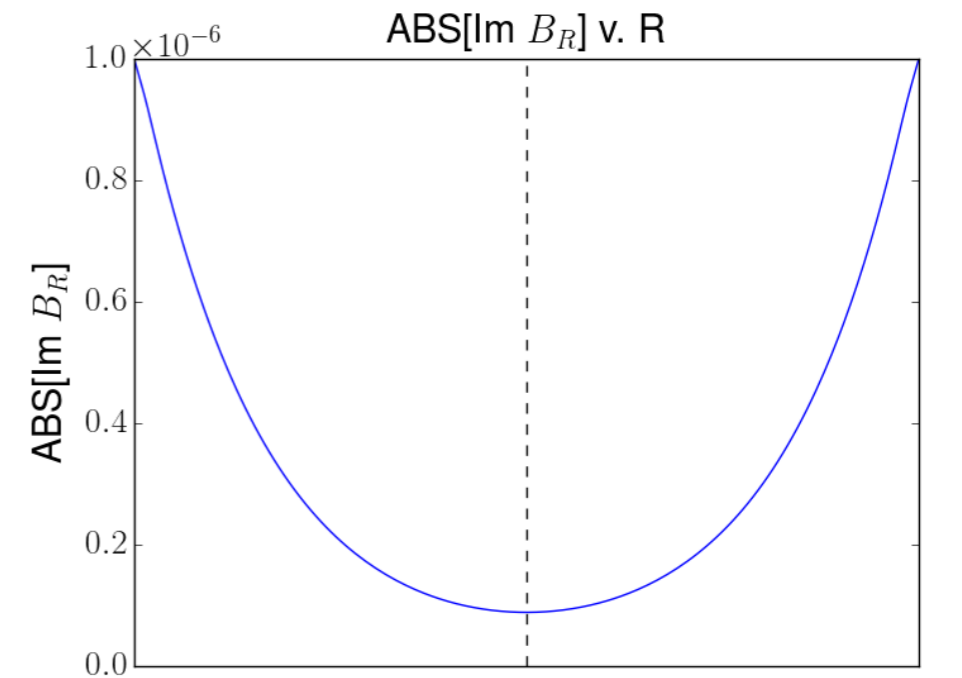
- $\mathbf{B}_\perp = \hat{\mathbf{z}} \times \nabla \psi$ and BC $\psi_1(R=a) = B_{nw}/k_\phi$
- Solution for system with $\psi_1(R=0) \neq 0$ (i.e. resistive evolution):

$$\psi_1(R, \phi) = \frac{-B_{nw}}{k_\phi} \frac{\cosh(k_\phi R)}{\cosh(k_\phi a)} (e^{ik_\phi \phi} + e^{-ik_\phi \phi})$$

- $B_{R,1}(\phi=0) = -iB_{nw}^* [\cosh(k_\phi R)/\cosh(k_\phi a)]$

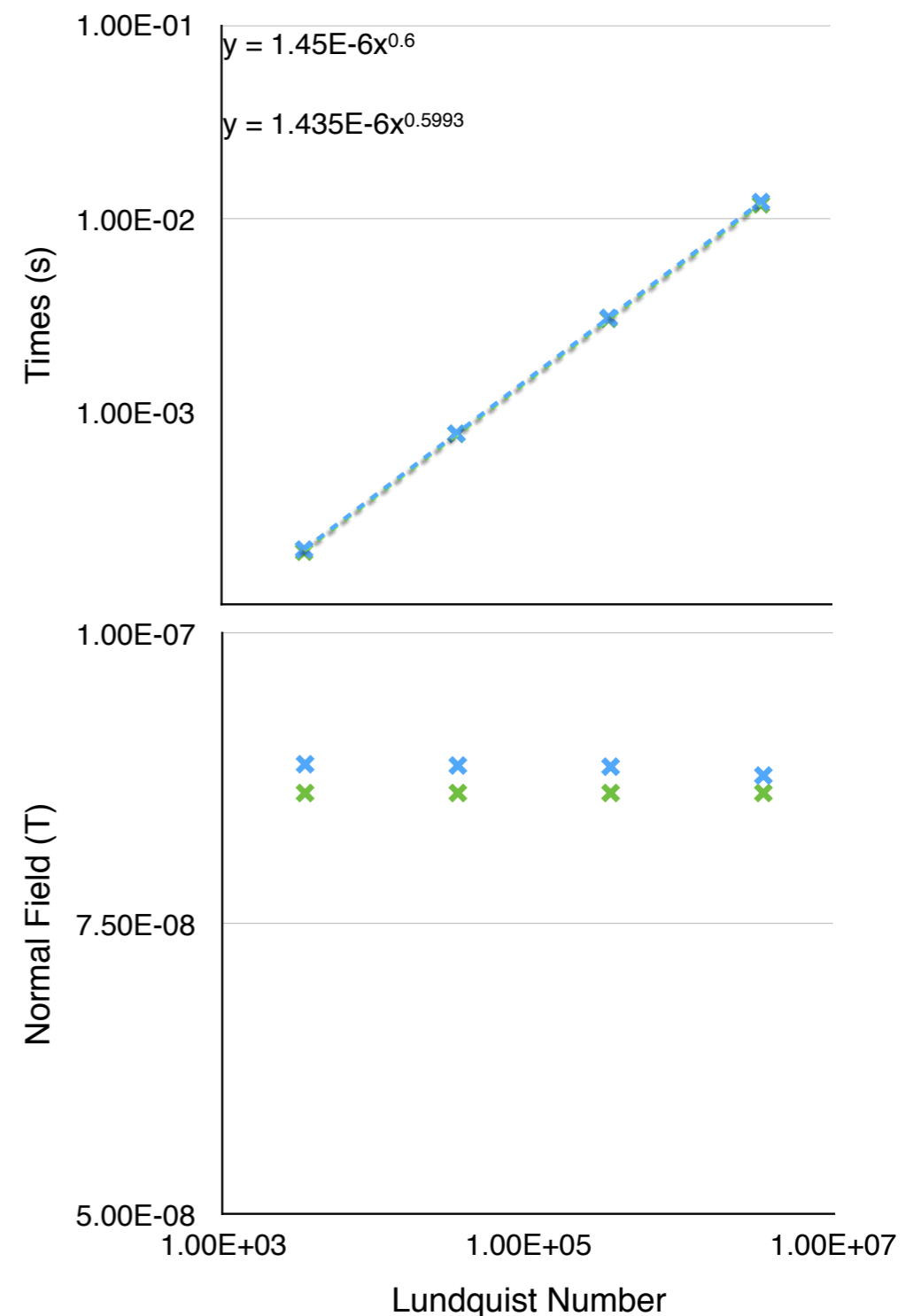
- $\text{Re}[B_{R,1}] \sim 0$

- $B_{\phi,1}(\phi=0) = B_{nw}^* [\sinh(k_\phi R)/\cosh(k_\phi a)]$



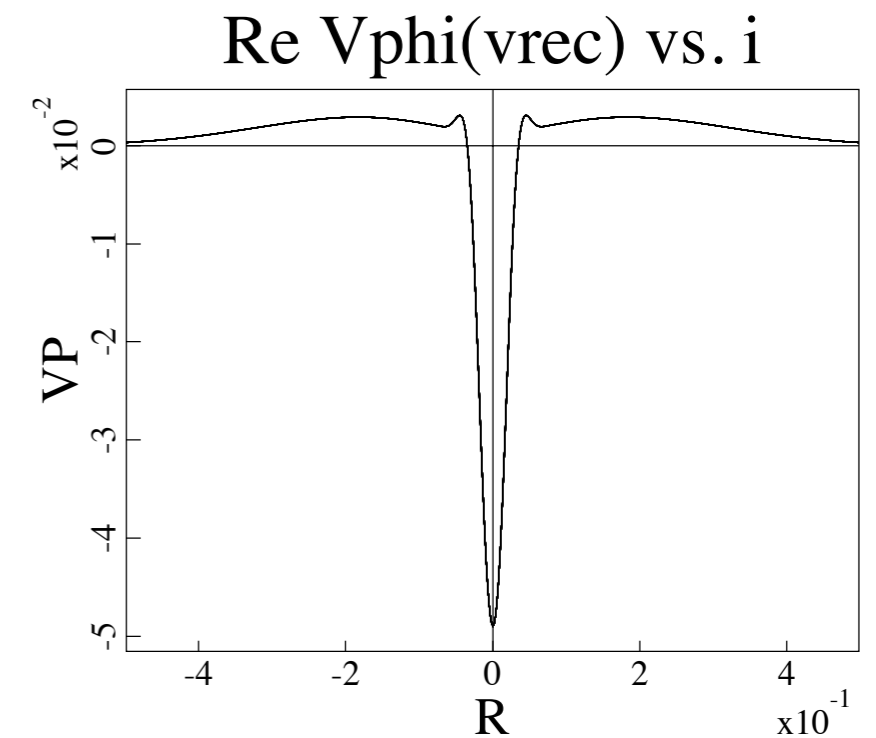
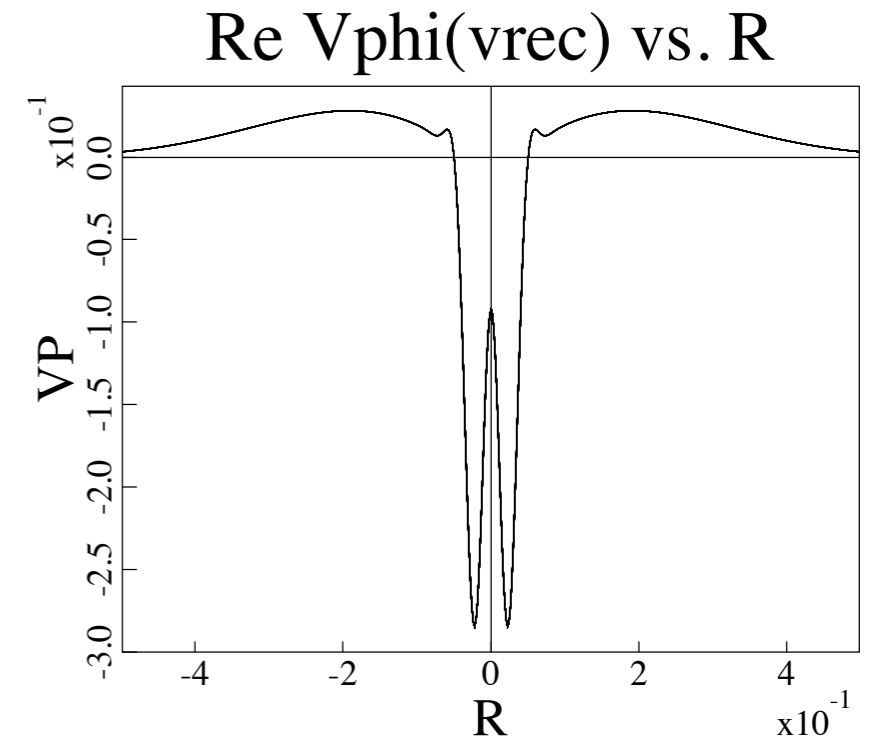
Parametric Results Agree with HK

- Varying Lundquist number gives outstanding agreement with analytical predictions
 - Time at maximum amplitude of $B_{R,1}$ (blue data) coincides with τ_T (green data)
 - *Traces lie on each other*
 - Varying B_{nw} has no effect on time of maximum amplitude of $B_{R,1}$
- Asymptotic value of $B_{R,1}(R=0)$ is independent of S as expected
 - Green data are HK predictions, blue data from NIMROD simulations



Alfvén Resonances Emerge for Increased Flows

- With $v_{\phi,0} = 10^4$, $\text{Re}(Q) \sim 3.19$ and we are in the I regime (shown in the top figure)
- Compared to the case with $v_{\phi,0} = 10^3$ (bottom figure), there are now two negative peaks in $\text{Re}(v_{\phi,1})$
- Due to an Alfvén Resonance
 - Where $(\mathbf{k} \cdot \mathbf{v})^2 = (k_{\phi} v_{A,\phi})^2$



Inertial Regime Has a Different Asymptotic State From the VR Regime

- Alfvén resonances creates smaller scale structure within the layer
- While top plot shows $\text{Re}[B_{R,1}(R=0)] \neq 0$, as $v_{\phi,0}$ is increased the normal field at the rational surface asymptotes to zero
- Bottom plot shows that the imaginary component of the normal field changes sign at the rational surface
- Essentially no tearing (reconnection) in this regime

